

# Mammalian heparanase: Gene cloning, expression and function in tumor progression and metastasis

ISRAEL VLodAVSKY<sup>1</sup>, YAEL FRIEDMANN<sup>1</sup>, MICHAEL ELKIN<sup>1</sup>, HELENA AINGORN<sup>1</sup>, RUTH ATZMON<sup>1</sup>,  
RIVKA ISHAI-MICHAELI<sup>1</sup>, MENACHEM BITAN<sup>1</sup>, ORIT PAPPO<sup>2</sup>, TUVIA PERETZ<sup>3</sup>, ISRAEL MICHAL<sup>3</sup>,  
LARISSA SPECTOR<sup>3</sup> & IRIS PECKER<sup>3</sup>

Departments of <sup>1</sup>Oncology and <sup>2</sup>Pathology, Hadassah-Hebrew University Hospital, Jerusalem 91120, and

<sup>3</sup>Insight, Rabin Science Park, Rehovot 76121, Israel

Correspondence should be addressed to I.V.; email: vlodavsk@cc.huji.ac.il

Heparan sulfate proteoglycans interact with many extracellular matrix constituents, growth factors and enzymes. Degradation of heparan sulfate by endoglycosidic heparanase cleavage affects a variety of biological processes. We have purified a 50-kDa heparanase from human hepatoma and placenta, and now report cloning of the cDNA and gene encoding this enzyme. Expression of the cloned cDNA in insect and mammalian cells yielded 65-kDa and 50-kDa recombinant heparanase proteins. The 50-kDa enzyme represents an N-terminally processed enzyme, at least 100-fold more active than the 65-kDa form. The heparanase mRNA and protein are preferentially expressed in metastatic cell lines and specimens of human breast, colon and liver carcinomas. Low metastatic murine T-lymphoma and melanoma cells transfected with the heparanase cDNA acquired a highly metastatic phenotype *in vivo*, reflected by a massive liver and lung colonization. This represents the first cloned mammalian heparanase, to our knowledge, and provides direct evidence for its role in tumor metastasis. Cloning of the heparanase gene enables the development of specific molecular probes for early detection and treatment of cancer metastasis and autoimmune disorders.

Heparan sulfate proteoglycans (HSPGs) are ubiquitous macromolecules associated with the cell surface and extracellular matrix (ECM) of a wide range of cells of vertebrate and invertebrate tissues<sup>1-6</sup>. The basic HSPG structure consists of a protein core to which several linear heparan sulfate (HS) chains are covalently attached. The HS chains are typically composed of repeating hexuronic and D-glucosamine disaccharide units that are substituted to a varying extent with N- and O-linked sulfate moieties and N-linked acetyl groups<sup>1</sup>. The ability of HS to interact with ECM macromolecules such as collagen, laminin and fibronectin, and with different attachment sites on plasma membranes indicates this proteoglycan is essential in the self-assembly and insolubility of ECM components, as well as in cell adhesion and locomotion<sup>3-5</sup>. HSPGs are prominent components of blood vessels<sup>6</sup>. In capillaries they are found mainly in the subendothelial basement membrane, where they support the vascular endothelium and stabilize the structure of the capillary wall. Cleavage of HS therefore plays a decisive part in the extravasation of blood-borne cells. In fact, expression of HS-degrading endoglycosidases, commonly called 'heparanases', correlates with the metastatic potential of mouse lymphoma, fibrosarcoma and melanoma cell lines<sup>7,8</sup>. Moreover, increased levels of heparanase were detected in sera<sup>9</sup> and urine of metastatic tumor-bearing animals and cancer patients (I.V. *et al.*, unpublished results). Treatment of experimental animals with heparanase inhibitors (for example, non-anticoagulant species of low-molecular-weight heparin and polysulfated saccharides) considerably reduced the incidence of lung metastases by melanoma, Lewis lung carcinoma and mammary adenocarcinoma cells<sup>9-11</sup>. Heparanase-inhibiting molecules also inhibit T cell-mediated

delayed-type hypersensitivity and experimental autoimmune encephalomyelitis and adjuvant arthritis<sup>12-14</sup>, reflecting a role in cell diapedesis and extravasation associated with inflammation and autoimmunity. Endoglycosidases, mainly endo- $\beta$ -D-glucuronidases, capable of partially depolymerizing HS chains, have been demonstrated in a variety of cells and tissues<sup>15</sup>. In addition to being involved in the remodeling of ECM and in the egress of cells from the vasculature, heparanases may regulate angiogenesis, tissue repair and lipid metabolism by releasing HS-bound growth factors and enzymes such as basic fibroblast growth factor (bFGF) and lipoprotein lipase<sup>16-18</sup>. Research on the involvement of heparanase in these processes has been handicapped by the lack of purified enzyme preparations and appropriate molecular probes and antibodies to explore a causative role for heparanase in normal and pathological processes.

Several species of heparanase have been purified from human platelets with molecular weights of 137 kDa (ref. 19), 50 kDa (ref. 20), and 32-40 kDa (ref. 21). The last was proposed to be an endoglucosaminidase consisting of four subunits, each closely related to the CXC chemokines connective tissue activating peptide-III and neutrophil activating peptide-2 (ref. 21). Sequences of three peptides derived from the platelet enzyme have been reported<sup>22</sup>. A 98-kDa heparanase has been purified from mouse melanoma and partially sequenced<sup>23</sup>. This sequence was later attributed to an endoplasmin-like contaminant<sup>15,24</sup>. No direct evidence for the biological function of any of these isolated enzymes was reported.

Here we describe the molecular cloning, expression and function of a human heparanase. For this, we have purified heparanase enzymes of about 50 kDa from human placenta<sup>25</sup> and

**Fig. 1** Nucleotide sequence and predicted amino acid sequence of human heparanase. **a**, Above, nucleotide sequence; below, predicted amino acid sequence. Right, numbers indicate the nucleotide residues and the amino-acid residues (italics). \*, potential N-glycosylation sites. The potential signal peptide region is underlined. **b**, Hydropathic curve, was calculated according to the Kyte-Doolittle method. Vertical axis, average hydropathy values over a window of 17 amino acids; horizontal axis, number of amino-acid residues. **c**, Genomic heparanase gene. Vertical rectangles, exons; horizontal line, introns and non-transcribed upstream and downstream sequences.

from a human hepatoma cell line (SK-hep-1). This led to the cloning and functional expression of a full-length mammalian heparanase cDNA. This is the first time, to our knowledge, that a mammalian HS-degrading enzyme has been cloned and expressed. The enzyme is synthesized as a latent protein of about 65 kDa that is then processed at the N terminus into a highly active form of about 50 kDa. The heparanase mRNA and protein are preferentially expressed in highly metastatic mouse and human cell lines and in biopsy specimens of human tumors. Overexpression of the heparanase cDNA in low or non-metastatic tumor cells conferred a high metastatic potential in experimental mice, resulting in an increased rate of mortality.

**Cloning of a unique mammalian heparanase gene**

We purified heparanase from a human hepatoma cell line (SK-hep-1) and from human placenta by sequential chromatographies on CM-Sepharose, heparin-Sepharose, ConA-Sepharose and Mono-S resin, as described<sup>25</sup>. Tryptic peptides derived from the purified preparation were separated by reverse phase HPLC and the most prominent peptides were isolated and subjected to amino acid sequencing. We used unique sequences to screen EST databases for homology to the corresponding back-translated DNA sequences. We identified two closely related EST sequences that were found to be identical. These two sequences were derived from cDNA clones 257548 and 260138 (I.M.A.G.E. Consortium) prepared from a cDNA library from placentas 8–9 weeks old. Both clones contained an insert of 1020 bp, which included an open reading frame of 973 bp followed by 27 bp of 3' untranslated region and a 20-bp polyA tail. We did not identify a translation start site (AUG). We cloned the missing 5' end by PCR amplification of DNA from placenta Marathon RACE cDNA composite. We obtained a 930-bp PCR fragment, partially overlapping with the identified 3' encoding EST clones. We called the entire cDNA cloned in PT3T7-Pac vector *Phpa*. The complete cDNA (*hpa*) is 1,758 bp long, and it contains an open reading frame that encodes a polypeptide of 543 amino acids (Fig. 1a) with a calculated molecular weight of 61,192 daltons. The heparanase enzymes of about 50 kDa isolated from human placenta and SK-hep-1 cells may thus represent a processed form of the native protein.

The hydropathic profile of the protein (Fig. 1b) indicates a hydrophobic amino acid stretch (Fig. 1a, underlined) at the N terminus. The homology of this stretch to known signal peptide sequences indicates that it could function as a signal peptide for secretion. Analysis of the heparanase amino acid sequence demonstrated two potential cleavage sites at positions 27–28 or 35–36 (Fig. 1a). As the N terminus of the purified recombinant protein was blocked, the exact cleavage site of the signal peptide could not be identified. A hydropathic plot (Fig. 1b) demonstrated a prominent hydrophilic region located between amino acids 110 and 170. The deduced amino-acid sequence indicated six potential N-glycosylation sites (Fig. 1a).

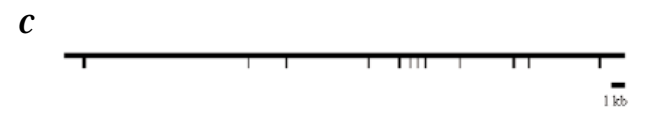
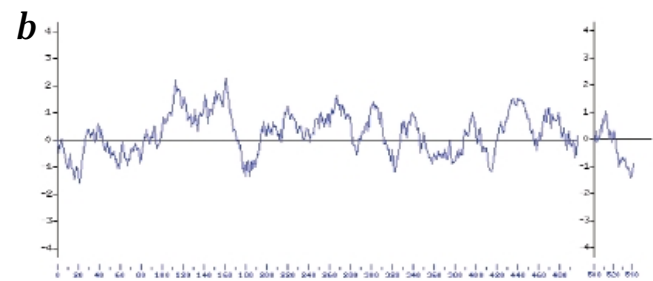
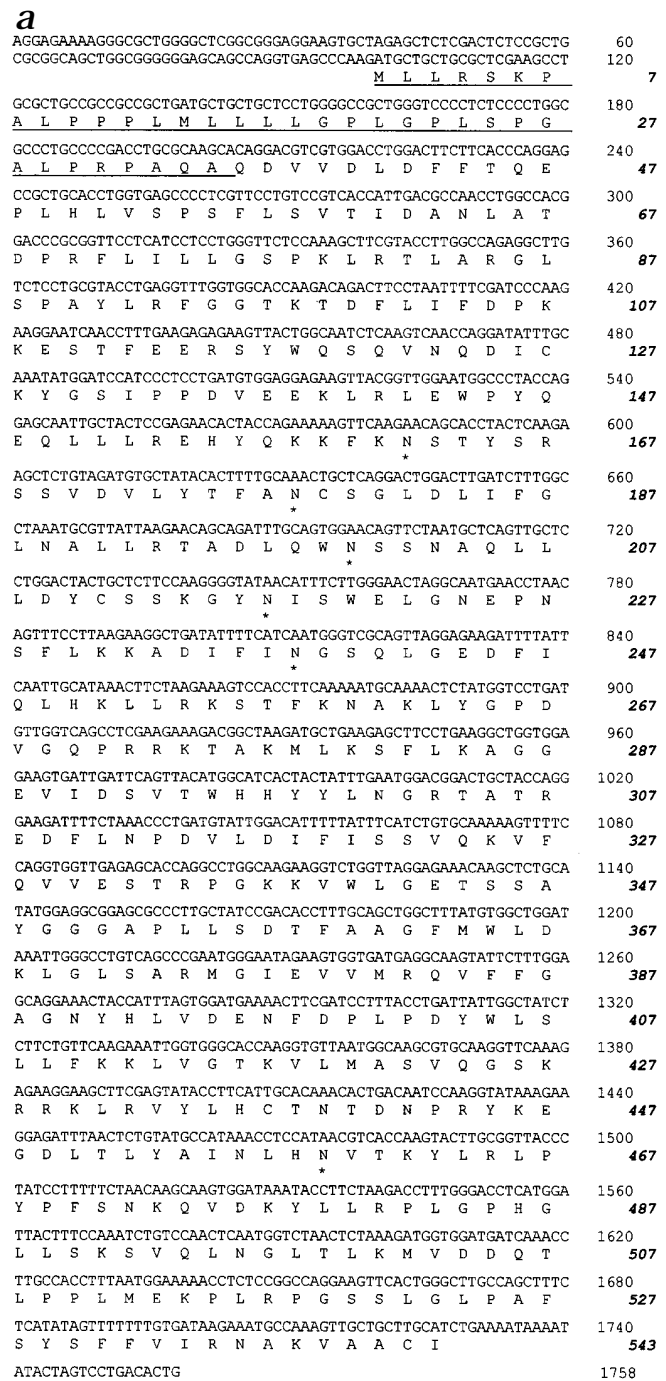
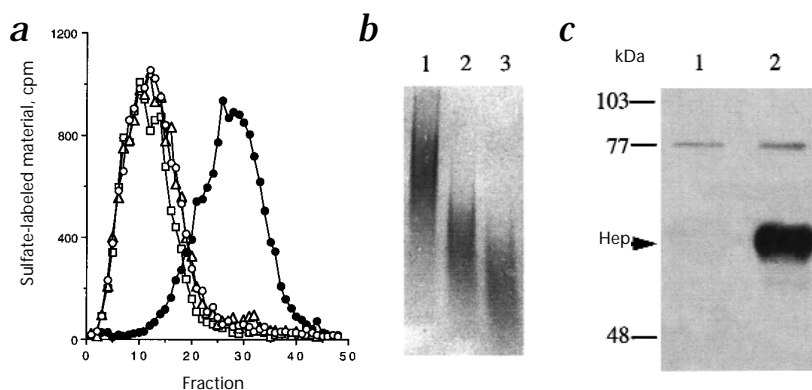


**Fig. 2** Expression of the *hpa* gene in a baculovirus expression system. **a**, Heparanase activity, by ECM assay. Conditioned medium of High Five cells infected with control (pF; ○) or *hpa*-containing virus (pF*hpa*; ●) were incubated with sulfate-labeled, ECM-derived HSPGs (peak I; △) in the absence (all symbols except □) or presence (□) of 5 µg/ml heparin. The incubation medium was then subjected to gel filtration over Sepharose 6B. Low-molecular-weight HS degradation fragments (peak II) are produced only during incubation with medium conditioned by pF*hpa*-infected cells. **b**, Heparanase activity, by gel shift assay. Bovine lung heparan sulfate (HS) was incubated in the absence and presence of partially purified heparanase produced by pF*hpa*-infected High Five cells. Degradation products were separated by 10% PAGE and stained with methylene blue<sup>24</sup>. Lane 1, HS substrate alone; lanes 2 and 3, HS incubated with recombinant heparanase for 3 and 6 h, respectively. **c**, Western blot analysis with monoclonal antibodies against heparanase. Lane 1, conditioned medium of High



Five cells infected with control, insert free-pF virus; lane 2, conditioned medium of insect cells infected with *hpa*-containing virus (pF*hpa*). Arrow, heparanase. Left margin, molecular weight markers.

### Genomic heparanase gene

We cloned the genomic region encoding *hpa* from a human genomic library. Three isolated plaques contained the entire coding region of *hpa*, except for a 2-kb DNA gap that was amplified by PCR from human genomic DNA. We analyzed the sequence of the entire genomic region of the *hpa* gene. The coding region from the first ATG to the stop codon spans 39,113 nucleotides. Comparison of the genomic sequence with that of *hpa* cDNA showed there are 12 exons separated by 11 introns (Fig. 1c). The analyzed sequence includes a 2.3-kb area upstream of the *hpa* coding region that contains the promoter. The human heparanase gene is on human chromosome 4, as determined by using a panel of monochromosomal human-CHO and human-mouse somatic cell hybrids.

### Functional expression of recombinant heparanase in insect cells

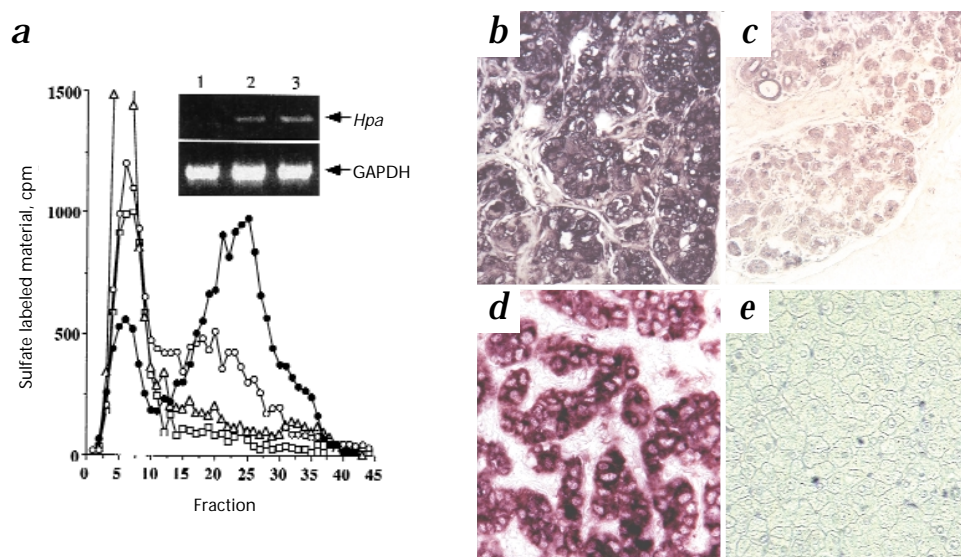
We assessed the ability of the *hpa* gene product to catalyze degradation of heparan sulfate *in vitro* by expressing the entire open reading frame of *hpa* in insect cells, using the baculovirus expression system. We infected monolayer cultures of High Five insect cells derived from *Trichoplusia ni* eggs with recombinant baculovirus containing the pFast*hpa* heparanase cDNA (pF*hpa*), or with control virus containing an insert-free plasmid (pF). Cell lysates or conditioned medium were then incubated for 18 hours at 37 °C, pH 6.2, with sulfate-labeled, ECM-derived HSPG (peak I), followed by gel filtration on Sepharose 6B. The substrate alone consisted almost entirely of intact, high-molecular-weight material eluted just after the void volume  $V_0$  (peak I, fractions 5–20,  $K_{av} < 0.2$ ). A similar elution pattern was obtained when the HSPG substrate was incubated with medium of cells infected with control virus (Fig. 2a). In contrast, incubation of the HSPG substrate with lysates or media of cells infected with *hpa*-containing virus resulted in a complete conversion of the high-molecular-weight substrate into low-molecular-weight labeled degradation fragments (peak II, fractions 25–35,  $0.5 < K_{av} < 0.75$ ; Fig. 2a). Conversion of the substrate (peak I) into peak II HS degradation fragments was abolished in the presence of excess heparin, an alternative substrate of the heparanase enzyme<sup>26</sup>. Labeled fragments eluted in peak II were shown to be degradation products of HS, as they were 500–600% smaller than intact HS side chains, resistant to further digestion with papain or chondroitinase ABC and were susceptible to deamination by nitrous acid<sup>7</sup>. The ability of the recombinant enzyme to degrade HS was also demon-

strated by the polyacrylamide gel shift assay<sup>24</sup>, showing an accelerated mobility of degradation products compared with the untreated HS substrate (Fig. 2b). These results demonstrate that heparanase activity is expressed by cells infected with baculovirus containing the human *hpa* gene. Similar results were obtained when intact, naturally produced, sulfate-labeled ECM was used as the substrate (data not shown). The recombinant enzyme is thus capable of degrading HS complexed to other constituents (that is, fibronectin, laminin and collagen) of the ECM, in a manner similar to that seen with highly metastatic tumor cells and activated cells of the immune system<sup>10,14</sup>. Partial purification of the recombinant heparanase enzyme by sequential chromatography of the conditioned medium over heparin-Sepharose and Superdex 75 columns demonstrated a predominant 65-kDa protein (not shown), consistent with the calculated molecular weight of the *hpa* gene product. Incubation of sulfate-labeled ECM for 2 hours at 37 °C, pH 6.0, with 1 µg of the purified preparation resulted in release of about 50% of the total ECM-associated radioactivity in the form of low-molecular-weight HS degradation fragments. Polyclonal and monoclonal antibodies raised against the purified enzyme detected a 65-kDa protein in western immunoblot analysis of crude preparations (Fig. 2c) and purified fractions of the recombinant enzyme produced by baculovirus-infected insect cells. The 65-kDa recombinant protein is glycosylated, as indicated by its retention on ConA-Sepharose, its apparent and calculated molecular weight, and the identification of six potential glycosylation sites. After deglycosylation by treatment with peptide N-glycosidase, the protein appeared as a band of about 58 kDa. This molecular weight corresponds to the deduced molecular mass (61,192 daltons) of the 543-amino-acid polypeptide encoded by the full-length *hpa* cDNA after cleavage of the predicted 3- to 4-kDa signal peptide. No further reduction in the apparent size of the N-deglycosylated protein was seen after concurrent O-glycosidase and neuraminidase treatment. Deglycosylation had no detectable effect on enzymatic activity (not shown).

### Preferential expression of the *hpa* gene in human tumors

We used semi-quantitative RT-PCR to evaluate the expression of the *hpa* gene by human breast carcinoma cell lines with different degrees of metastasis<sup>27</sup>. Although in nonmetastatic MCF-7 breast carcinoma cells, the expected 585-bp PCR product of the *hpa* cDNA was not detected (Fig. 3a, inset, lane 1), moderate (MDA

**Fig. 3** Preferential expression of heparanase in human breast and hepatocellular carcinomas. **a**, Human breast carcinoma cell lines with different degrees of metastasis tested for expression of the *hpa* gene (inset) and heparanase activity. MCF-7 ( $\Delta$ ), MDA-231 ( $\circ$ ) or MDA-435 ( $\bullet$ ) cells or control medium alone ( $\square$ ) were incubated in contact with sulfate-labeled ECM. Labeled degradation products released into the incubation medium were analyzed by gel filtration on Sepharose 6B. Inset, Total RNA assessed by RT-PCR using primers specific for heparanase (top) and GAPDH (bottom). Lane 1, nonmetastatic MCF-7 cells; lane 2, moderately metastatic MDA-231 cells; lane 3, highly metastatic MDA-435 cells. **b-e**, *In situ* hybridization of *hpa* mRNA in human breast and hepatocellular carcinomas. Hybridization with *hpa* riboprobes on paraffin-embedded human specimens derived from invasive ductal carcinoma of breast (**b**) and hepatocellular carcinoma (**d**) compared with specimens derived from normal breast



and adult liver (**e**) tissues. Hybridization of the same specimens with the *hpa* sense riboprobe yielded no staining.

(**c**) and adult liver (**e**) tissues. Hybridization of the same specimens with the *hpa* sense riboprobe yielded no staining.

231; Fig. 3a, inset, lane 2) and highly (MDA 435; Fig. 3a, inset, lane 3) metastatic breast carcinoma cell lines showed a substantial increase in *hpa* gene expression. The differential pattern of the *hpa* gene expression correlated with the pattern of heparanase activity. MCF-7 cells showed little or no heparanase activity, whereas MDA-231 and MDA-435 cells, known for their moderate and high metastatic potential in nude mice<sup>27</sup>, showed moderate and high heparanase activity (Fig. 3a).

We used sense and antisense deoxygenin-labeled *hpa* RNA probes to screen archival paraffin-embedded human breast tissue for expression of the *hpa* gene transcripts. We analyzed four specimens of normal breast tissue (reduction mammoplasty) and five specimens of infiltrating duct carcinoma with evidence of vascular invasion and lymph node metastases. Hybridization of the heparanase antisense riboprobe to invasive duct carcinoma tissue sections resulted in a massive positive staining localized specifically to the carcinoma cells (Fig. 3b). Hybridization of sections derived from the same specimen with the *hpa* sense riboprobe yielded no staining. The *hpa* gene was also expressed in areas adjacent to the carcinoma showing fibrocystic changes (not shown). Normal breast tissue derived from reduction mammoplasty did not express the *hpa* transcript, yielding the same staining both with the antisense (Fig. 3c) and sense probes. An intense expression of the *hpa* gene was also found in tissue sections derived from human hepatocellular carcinoma specimens (Fig. 3d), but not in normal adult liver tissue (Fig. 3e). Furthermore, tissue specimens derived from adenocarcinoma of the ovary, squamous cell carcinoma of the cervix and colon adenocarcinoma showed intense staining with the *hpa* RNA probe, compared with very weak staining of the *hpa* mRNA in the respective nonmalignant control tissues (not shown).

There was also preferential expression of heparanase in human tumors compared with that of the corresponding normal tissue, seen by immunohistochemical staining of paraffin-embedded sections with monoclonal antibodies against heparanase. We did immune staining of formalin-fixed, paraffin-embedded sections from colectomy specimen resected for adenocarcinoma and a liver metastasis resected from the same patient. Positive cytoplasmic and cell surface staining was

found in neoplastic cells of the colon carcinoma (Fig. 4c) and in dysplastic epithelial cells of a tubulovillous adenoma found in the same specimen (Fig. 4b). There was little or no staining of the 'normal-looking' colon epithelium located away from the carcinoma (Fig. 4a). There was an intense immunostaining of colon adenocarcinoma cells that had metastasized into the liver compared with that of the surrounding normal liver tissue (Fig. 4d).

#### Involvement of heparanase in tumor metastasis

We have studied a pair of murine T-lymphoma cell lines, highly metastatic ESb cells and their non-metastatic parental Eb cells<sup>7</sup>. ESb cells were derived from a spontaneous highly metastatic variant of the chemically induced T lymphoma L5178Y(Eb) of DBA/2 mice that arose most likely after fusion of Eb cells with a host macrophage<sup>28</sup>. ESb cells express heparanase activity, whereas Eb do not<sup>7</sup>, consistent with a differential expression of the mouse *hpa* mRNA by these sublines (Fig. 5a, top). We determined whether introduction of the *hpa* gene into Eb cells would confer a metastatic behavior on these cells. For this, we transfected Eb cells with a full-length human *hpa* cDNA using a pcDNA3 expression plasmid. We selected stably transfected, neomycin-resistant cells and tested them for expression of the heparanase mRNA and enzyme activity. RT-PCR analysis showed that the cells expressed high levels of *hpa* mRNA (Fig. 5a, bottom) and high heparanase activity, as indicated by release of characteristic sulfate-labeled HS degradation fragments from intact subendothelial ECM (Fig. 5b). Heparanase activity could not be detected in Eb lymphoma cells transfected with a control pcDNA3 plasmid lacking the heparanase cDNA insert (Fig. 5b). We injected these *hpa*- and mock-transfected Eb cells subcutaneously into DBA/2 mice and tested mice for survival time and liver metastases. All mice ( $n = 22$ ) injected with cells transfected with control pcDNA3 plasmid alone survived during the first 4 weeks of the experiment, in contrast to the 50% mortality in mice inoculated with Eb cells transfected with the *hpa*-containing expression plasmid (Fig. 5c). Of the mice inoculated with *hpa*-expressing Eb cells, 90% died by day 34, whereas 60% of the mice inoculated with mock-transfected cells survived at that time. We examined mice for liver colonization at various times.

The livers of mice inoculated with *hpa*-transfected cells were infiltrated with numerous Eb lymphoma cells, as was evident both by macroscopic evaluation of the liver surface and microscopic examination of tissue sections. Eb cells were mainly in the liver sinusoids, and were also in portal tracts and around and inside blood vessels (Fig. 5e). In contrast, metastatic lesions could not be detected by gross examination of the liver of mice inoculated with mock-transfected, control Eb cells. Few or no lymphoma cells infiltrated the liver tissue (Fig. 5d). In a different model of tumor metastasis, transient transfection of the heparanase gene into B16-F1 mouse melanoma cells with low metastatic potential followed by intravenous inoculation resulted in a 400–500% increase in lung metastases (data not shown).

#### Latent and active forms of the heparanase protein

We constructed a mammalian expression vector to drive the expression of the heparanase gene in CHO cells and human 293 kidney fibroblasts. We assessed transient and stable expression of heparanase in these cells by western blot analysis and measurements of heparanase activity in cell lysates and conditioned medium. We found a major band of about 50 kDa and a minor band of about 65 kDa in lysates of transfected CHO cells (Fig. 6a, inset). In contrast, mainly the high-molecular-weight form was detected in the conditioned medium of several stable transfected CHO clones (Fig. 6a, inset). Perhaps the approximately 65-kDa protein represents a heparanase precursor, whereas the 50-kDa protein is a processed or mature form. In an attempt to compare the specific activity of the two forms, we estimated the amounts of the heparanase protein in cell lysates and conditioned medium by SDS-PAGE and western blot analysis using monoclonal antibodies against heparanase. We used the purified recombinant enzyme produced in insect cells as a quantitative standard. We then tested various concentrations of the two different forms for heparanase activity, using sulfate labeled ECM as a substrate. A high activity (release of 80% of the total ECM associated radioactivity in the form of HS degradation fragments) was expressed by the approximately 50-kDa cell lysate enzyme already at an estimated concentration of about 1 ng/ml heparanase produced by  $2.5 \times 10^4$  cells (Fig. 6a), whereas a similar activity required about 100 ng/ml of the 65-kDa precursor enzyme secreted into the culture medium. This result reflects an increase of approximately 100-fold in the specific activity of the N-terminally processed enzyme compared with that of the latent form. In the same conditions, lysates of  $2.5 \times 10^6$  mock-transfected CHO cells failed to express detectable heparanase protein and activity (not shown), indicating that CHO cells overexpressing the recombinant enzyme are at least 100-fold more active than the mock-transfected CHO cells.

Next, we examined the ability of intact mammalian cells to convert the recombinant enzyme of about 65 kDa produced in the baculovirus expression system into a mature, processed form. For this, we incubated  $5 \times 10^6$  human bladder carcinoma cells for 4 hours at 37 °C with the recombinant enzyme. The cells were centrifuged and the supernatants assessed by SDS-PAGE

and western blot analysis. In these conditions, nearly 40% of the recombinant enzyme of about 65 kDa was converted into a form of about 50 kDa (Fig. 6b, lane 1).

#### Discussion

An endoglycosidase activity degrading heparan sulfate (HS) was first described in human placenta in 1979 (ref. 29). Since then, the enzyme has been identified in a variety of normal and malignant cells and tissues, among which are skin fibroblasts, cytotrophoblasts, hepatocytes, CHO cells, endothelial cells, platelets, mast cells, neutrophils, macrophages, T and B lymphocytes, lymphoma, melanoma, and carcinoma cells<sup>7–15,25,30–37</sup>. There have been several attempts to purify heparanase, but purification of the enzyme to homogeneity has been extraordinarily difficult, due to the extremely low abundance and unstable nature of the enzyme(s), and the lack of a convenient quantitative assay. Different species of heparanase may exist. For example, platelets may produce three HS degrading enzymes, with different molecular masses and substrate specificities<sup>19–22</sup>. Although it is generally accepted that heparanases expressed by circulating cells of the immune system and by metastatic cancer cells are important in the egress of blood-borne cells from the vasculature<sup>9–14</sup>, progress in studying their importance in health and disease has been handicapped by the lack of molecular probes and by conflicting and sometimes misleading results. For example, antibodies raised against a purified melanoma heparanase were later shown to recognize a 98-kDa endoplasmic-like protein<sup>15,24</sup>. Platelet-derived  $\beta$ -thromboglobulin preparations were reported to express HS degrading endoglycosaminidase activity<sup>21</sup>. However, the ability of this preparation to cleave a well-defined heparin octasaccharide pointed to glucuronidic linkages as the site of cleavage<sup>31</sup>, characteristic of heparanase enzymes isolated from a variety of sources, including platelets<sup>20</sup>. Whether platelets also contain a low-molecular-weight form of heparanase, identical to the CXC-chemokines, connective tissue-activating peptide-III and neutrophil-activating peptide-2, is still unresolved. A single cell type (CHO cells) may contain several heparanases with different substrate specificities<sup>30</sup>. Comparison of heparanases from mouse melanoma, mouse macrophages and human platelets has indicated, however, that the enzymes are very similar<sup>15</sup>. Different enzyme preparations derived from human platelets, hepatoma and placenta have similar substrate recognition properties<sup>31</sup>. Moreover, as described here, sequence analysis of peptides derived from purified preparations of the human hepatoma and placenta enzymes led to the molecular cloning and expression of a single gene. The reported sequences

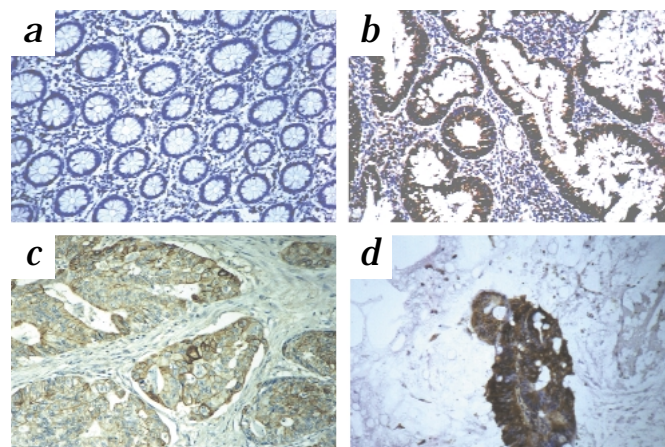


**Fig. 4** Preferential immunohistochemical staining of heparanase in a colonic polyp, primary and metastatic human colon adenocarcinoma. Immunostaining, with monoclonal antibodies against heparanase, of paraffin-embedded tissue specimens derived from colon epithelium removed from a normal region located away from the neoplastic lesion (**a**), tubulovillous adenoma (**b**), primary human colon adenocarcinoma (**c**), and colon carcinoma metastasized to the liver (**d**).

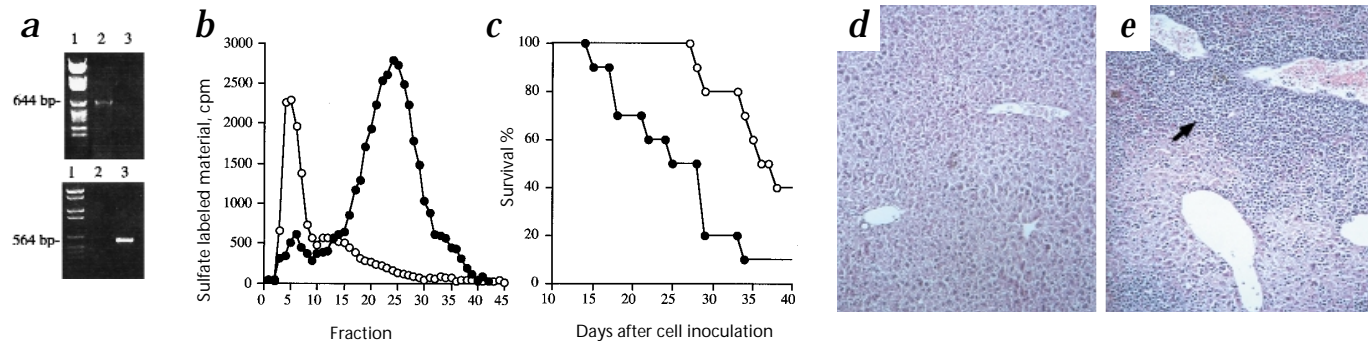


**Fig. 5** Overexpression of heparanase in non-metastatic Eb T-lymphoma cells leads to liver metastasis and accelerated mortality. **a**, Top, RT-PCR of non-metastatic murine Eb-lymphoma cells and the highly metastatic ESb variant cells, to assess expression of the *hpa* mRNA using mouse-specific *hpa* primers amplifying a 644-bp cDNA segment. Lane 1, DNA molecular weight markers; lane 2, ESb cells; lane 3, Eb cells. Bottom: Eb cells transfected with a full-length human *hpa* cDNA using pcDNA3 expression plasmid. Pooled populations of neomycin-resistant, stably transfected cells were tested for expression of the *hpa* mRNA using human-specific *hpa* primers. Lane 1, DNA molecular weight markers; lane 2, cells transfected with control plasmid alone; lane 3, cells transfected with plasmid containing *hpa*. **b**, Heparanase activity of Eb cells transfected with control plasmid alone (○) or with plasmid containing *hpa* (●) were

incubated with sulfate-labeled ECM. Labeled degradation fragments released into the incubation medium were analyzed by gel filtration over Sepharose 6B. **c–e**, Mortality and liver metastasis in DBA/2 mice inoculated with Eb cells transfected with control vector alone or plasmid containing *hpa* ( $n = 22$  mice per group). **c**, Mortality. ○, control vector alone; ●, plasmid containing *hpa*. **d**, infiltration of the liver tissue by lymphoma cells. On day 28, two mice of each group (with primary tumors of about 1.5 cm<sup>3</sup>) were killed and liver tissue specimens were processed for histological examination. Sections of paraffin-embedded tissue specimens were stained with hematoxylin and eosin. **d** and **e**, inoculation with mock-transfected Eb cells. **e**, inoculation with *hpa*-transfected Eb cells (arrow). The experiment was terminated on day 40, when the primary tumors reached an average size of about 4.5 cm<sup>3</sup>.

of three peptides derived from a purified platelet enzyme<sup>22</sup> are also included in the sequence in Fig. 1. These results and the lack of homologous sequences in the DNA and protein data banks indicate that heparanase enzymes from different sources are very similar, if not identical. In support of this, cDNA-specific primers synthesized on the basis of the newly identified, full-length heparanase cDNA detect the same mRNA fragment, determined by nucleotide sequence, regardless of the source and tissue of origin, whether normal (neutrophils, megakaryocytes and keratinocytes) or malignant (breast carcinoma, metastatic melanoma, myeloid leukemia) (I.V. *et al.*, unpublished results). Moreover, cloning of the mouse heparanase gene shows a high homology (more than 80%) with the human enzyme, indicating that the gene is highly conserved.

The apparent molecular size of the recombinant enzyme produced in the baculovirus expression system was about 65 kDa. This heparanase polypeptide contains six potential N-glycosylation sites. After deglycosylation by treatment with peptide N-glycosidase, the protein appeared as a band of about 58 kDa. The genomic locus that encodes heparanase spans about 40 kb. It is composed of 12 exons separated by 11 introns, and is on human chromosome 4. A more accurate localization will verify whether the gene is located in the vicinity of other genes involved in inflammation and cancer progression. The promoter region upstream the *hpa* gene has been identified. We are now investigating the regulation of *hpa* gene expression at the transcription level in relation to its role in health, disease and embryonic development.

Unlike the baculovirus enzyme, expression of the full-length heparanase polypeptide in CHO cells yielded a major protein of about 50 kDa and a minor protein of about 65 kDa in cell lysates. There was preferential release of the approximately 65-kDa form into the culture medium in some of the transfected CHO clones. Semi-quantitative gel filtration assay showed that the 50-kDa enzyme is about 100-fold more active than the 65-kDa form. In a new colorimetric assay that monitors the amount of newly

formed HS cleavage products, 1 unit of heparanase activity produces 1 μmole of products per minute per mg protein. On the basis of this assay, we estimate the specific activity of the purified 50-kDa recombinant enzyme expressed by *hpa*-transfected CHO cells to be 0.3 units. This value is in the range of the specific activities of other glycosyl hydrolases. The specific activity of the 65-kDa recombinant enzyme produced in the baculovirus expression system is at least 1000-fold lower. These results indicate that the 50-kDa protein is a mature processed form of a latent heparanase precursor. As indicated by the hydropathic plot, a hydrophilic region is located between amino acids 110 and 170. A hydrophilic peak is predicted around amino acid 160. This region is likely to be exposed and therefore accessible to proteases. N-Terminal amino-acid sequencing of the platelet enzyme, recently purified and sequenced in our laboratory, indicates that the actual cleavage site is glu<sub>157</sub>-lys<sub>158</sub>. This conversion can be readily demonstrated after incubation of the full-length recombinant enzyme with intact tumor cells. The nature of the cellular, possibly membrane-bound enzyme(s), involved in processing and activation of the latent heparanase enzyme is being investigated. The activity ascribed to the 65-kDa recombinant heparanase produced by *hpa*-infected insect cells or secreted by some *hpa*-transfected CHO clones is due to minor processing and presence of residual 50-kDa enzyme in these preparations, indicating that the unprocessed 65-kDa enzyme may lack heparanase activity altogether.

Conversion of a proenzyme into an active enzyme provides a likely means by which heparanase-mediated cleavage of HS is regulated at the protein level, in physiological and pathological conditions. A proteolytic activation of a pro-enzyme is a common feature of enzymes (for example, matrix metalloproteinase and plasminogen activators) involved in degradation of ECM proteins and in cell invasion<sup>38–40</sup>. It now seems that the same principle is true for endoglycosidic enzymes that degrade HS and other cellular and extracellular glycosaminoglycans (GAGs). Proteases may thus regulate the degradation of GAG compo-

nents through activation of latent GAG degrading enzymes, and, as demonstrated<sup>41</sup>, better exposure of GAG side chains embedded in the ECM to a specific polysaccharide-degrading enzyme. Cell migration and matrix degradation of complex supramolecular structures such as basement membranes and ECM involve the concerted, sequential action of proteases and GAG-degrading enzymes<sup>41</sup>. As with the well-documented importance of matrix metalloproteinases in normal development and tumor progression<sup>38,39</sup>, cloning and expression of the mammalian heparanase gene is expected to add a new insight to our understanding of processes involving cell migration and ECM degradation and remodeling.

Expression of the heparanase gene and protein correlated with the metastatic potential of several human and mouse cell lines such as breast, bladder, prostate, melanoma and T-lymphoma (Figs. 3 and 5 and I.V. *et al.*, unpublished results). Preferential expression of the heparanase gene and protein was also found in biopsy specimens of human tumors, compared with that of the respective normal tissues. Only three examples (breast carcinoma, colon carcinoma, hepatocellular carcinoma) are presented here, but similar results were obtained with a variety of other tumors (metastatic melanoma, cervix carcinoma, neuroblastoma, mesothelioma, endothelioma), indicating both diagnostic and prognostic applications. Heparanase activity was detectable in the urine of some metastatic cancer patients, in contrast to the undetectable levels in normal donors (ref. 42 and I.V. *et al.*, unpublished observations). Heparanase might preferentially and readily cross the glomerular basement membrane barrier by virtue of its ability to degrade HS and thus destroy its perselectivity properties. Immunohistochemical staining of cultured cells and tissue specimens (Fig. 4c) indicates that the enzyme is found both as an intracellular and cell-surface protein. It is also secreted by highly metastatic tumor cells, activated T-lymphocytes, mast cells, platelets and neutrophils<sup>7,8,14</sup>. A detailed study of the enzyme intracellular localization, membrane association and secretory properties has been initiated.

Heparanase-inhibiting molecules (for example, non-anticoagulant species of heparin and polysulfated polysaccharides) inhibit lung colonization of blood-borne tumor cells<sup>9-11</sup>. Although the anti-metastatic activity of these molecules correlated with their anti-heparanase activity, other explanations (that is, effect on cell adhesion) could not be eliminated. More convincing evidence for a direct role of heparanase in tumor metastasis is

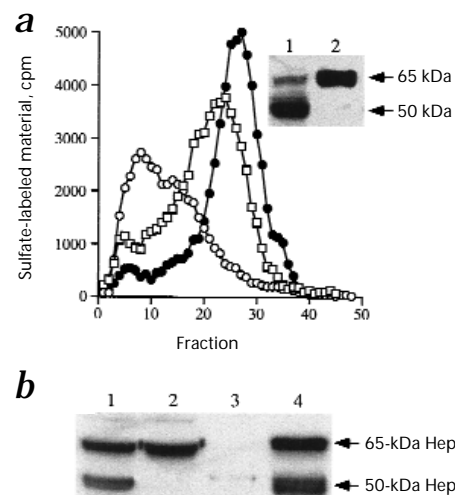
provided by the conversion of Eb T-lymphoma cells from non-metastatic to metastatic behavior after stable transfection and overexpression of the heparanase gene. The highly metastatic nature of the transfected cells was indicated by the massive infiltration of the mouse liver with lymphoma cells and the accelerated mortality rate of the tumor-bearing mice. Likewise, transient transfection of the heparanase gene into B16-F1 mouse melanoma cells with low metastatic potential followed by intravenous inoculation resulted in an increase of 400–500% in lung colonization compared with that of mock-transfected cells. The ability of heparanase to induce a metastatic phenotype is being tested in an experimental system involving surgical excision of the primary tumor long before it can kill the host.

In addition to being involved in cell invasion, HSPGs may be involved in many cellular processes, including cell adhesion, differentiation and proliferation<sup>1-6,42,43</sup>. Most of the identified functions are attributed to interaction of the GAG chains with protein ligands such as lipoprotein lipase, fibronectin and various members of the heparin-binding growth factor family<sup>3-5,18,42,43</sup>. HSPGs function not only as co-receptors for bFGF, mediating receptor dimerization and signaling<sup>44,45</sup>, but also serve as bFGF reservoirs in the ECM (refs. 17,42,43,46). Heparanase may thus elicit an indirect angiogenic response by means of releasing highly active HS-bFGF complexes from storage in the ECM and tumor microenvironment<sup>17,42,43,47</sup>. Such a role was demonstrated in studies with platelets, neutrophils and lymphoma cells<sup>16</sup>. Characterization of the heparanase protein is expected to enable the development of specific inhibitors and neutralizing antibodies that will halt the ability of metastatic tumor cells and activated cells of the immune system to leave the circulation and reach their target organs. These inhibitors may also suppress angiogenesis through inhibition of heparanase mediated release of HS-sequestered angiogenic heparin-binding factors.

## Methods

**Cells.** The methylcholanthrene-induced nonmetastatic Eb (L5178Y) T-lymphoma cells (clone 737) were provided by V. Schirmacher (DKFZ, Heidelberg, Germany) (refs. 7,28). The cells were routinely transplanted as ascites tumors in syngeneic female DBA2/J mice. Alternatively, they were grown in RPMI 1640 (Life Technologies) supplemented with  $\beta$ -mercaptoethanol ( $5 \times 10^{-5}$  M) and 10% FCS (ref. 7). Subcutaneous inoculation of  $2 \times 10^5$  cells per DBA/2 mouse results in formation of a primary tumor. Unlike the highly metastatic ESb variant, more than 90% of the mice

**Fig. 6** Processing of a 65-kDa proenzyme into a highly active 50-kDa heparanase enzyme. **a**, Heparanase derived from the conditioned medium (mainly the approximately 65-kDa form) and lysates (mostly the approximately 50-kDa form) of a selected *hpa*-transfected CHO clone, were incubated with sulfate-labeled ECM. Labeled degradation fragments released into the incubation medium were analyzed for heparanase activity by gel filtration over Sepharose 6B. Filled circles, ~1 ng cell lysate heparanase; open symbols, approximately 1 ng (circles) and 50 ng (squares) heparanase protein secreted into the culture medium. Lysates of mock-transfected CHO cells failed to express detectable heparanase activity at concentrations as high as  $2.5 \times 10^6$  cells/ml. Inset, CHO cells were transfected with a full-length *hpa* cDNA inserted in a pcDNA3 expression plasmid. Cell lysates (lane 1) and medium (lane 2) of a selected neomycin resistant clone were assessed by western immunoblot analysis with monoclonal antibodies against heparanase. **b**, Recombinant 65-kDa enzyme produced by baculovirus infected insect cells was incubated with or without intact human bladder carcinoma cells. The incubation medium was assessed by western blot analysis with monoclonal antibodies against heparanase. Lane 1, recombinant, approximately 65-kDa enzyme incubated with human bladder carcinoma cells; lane 2, recombinant, approximately 65-kDa enzyme produced in insect cells; lane 3, supernatant of control human bladder carcinoma cells; lane 4, lysates of *hpa*-transfected human 293 cells. Hep, heparanase.



survive as long as 20 days after cell inoculation, with few or no liver metastases<sup>28</sup>. DBA/2J and C57BL mice were purchased from Harlan Laboratories (Jerusalem, Israel) and maintained in accordance with current regulations and standards of the United States Department of Agriculture, Department of Health and Human Services and the NIH. All animal procedures were approved by our local institutional animal care and use committee. Tumor-bearing mice were killed by cervical dislocation and were not kept alive after they developed a maximum tumor size of about 4.5 cm<sup>3</sup>. The human breast carcinoma cell lines MCF-7 (adenocarcinoma), MDA-MB-231 (adenocarcinoma) and MDA-MB-435 (ductal carcinoma) were provided by R. Stern (Department of Pathology, University of California, San Francisco). The invasive properties of these cell lines were determined after injection of the cells into the mammary pads of nude mice with or without Matrigel<sup>49</sup>. Cells were cultured in DMEM (4.5 g glucose per liter) containing 10% fetal calf serum. SK-hep-1 human hepatoma cells, 293 human kidney fibroblasts, 5637 human bladder carcinoma cells and Chinese hamster ovary cells (CHO) were obtained from ATCC (Rockville, Maryland). Cells were maintained at 37 °C in a 10% CO<sub>2</sub> humidified incubator. Cells were dissociated with a solution of 0.05% trypsin, 0.02% EDTA, 0.01 M sodium phosphate, pH 7.4, and were subcultured at a 'split' ratio of 1:5.

**Purification of heparanase from a human hepatoma cell line and human placenta.** Sk-Hep-1 human hepatoma cells were applied as a source for purification of a human tumor derived heparanase, as described for human placenta<sup>25</sup>, with some modifications. Cells grown in suspension to a density of 1 × 10<sup>6</sup> cells/ml were collected and lysed. The heparanase enzyme was purified more than 240,000-fold by sequential chromatographies on CM-Sephadex; heparin-Sepharose; ConA-Sepharose and HPLC Mono-S cation exchange chromatography, as described<sup>25</sup>. Active fractions were pooled and separated by 7% SDS-PAGE, followed by transfer to a polyvinylidene difluoride membrane for sequence analysis. The N terminus of the protein was blocked. Another portion of the purified protein was digested with trypsin and the generated peptides were separated on a reverse-phase C4 column. Selected homogeneous peaks were subjected to sequence analysis using an applied Biosystem model 470A sequencer. A similar procedure was applied for purification and sequence analysis of heparanase from human placenta.

**Preparation of dishes coated with ECM.** Cultures of bovine corneal endothelial cells were established from steer eyes and maintained in DMEM (1 g glucose/liter) supplemented with 5% newborn calf serum and 10% FCS, as described<sup>49</sup>. Recombinant human bFGF (provided by Takeda Chemical Industries, Osaka, Japan) was added (1 ng/ml) every other day during the phase of active cell growth<sup>49</sup>. Bovine corneal endothelial cells (second to fifth passage) were plated into 35-mm tissue culture plates at an initial density of 2 × 10<sup>5</sup> cells/ml and cultured as described above, except that 4% dextran T-40 was included in the growth medium. Na<sub>2</sub><sup>35</sup>SO<sub>4</sub> (25 μCi/ml) was added on days 2 and 5 after seeding and the cultures were incubated with the label without medium change. On day 12, the subendothelial ECM was exposed by dissolving the cell layer with PBS containing 0.5% Triton X-100 and 20 mM NH<sub>4</sub>OH, followed by four washes with PBS (ref. 49). The ECM remained intact, free of cellular debris and firmly attached to the entire area of the tissue culture dish<sup>49</sup>. To prepare soluble sulfate labeled proteoglycans, the ECM was digested with 50 μg/ml trypsin overnight at 37 °C. The digest was concentrated by reverse dialysis, applied onto a Sepharose CL-6B column and the high-molecular-weight material (K<sub>av</sub> < 0.2, peak I) was collected. More than 80% of the labeled material was composed of HSPGs (ref. 7).

**Heparanase activity.** Cell lysates, conditioned media or intact cells (1 × 10<sup>6</sup> cells per 35-mm dish) were incubated for 18 h at 37 °C, pH 6.2–6.6, with <sup>35</sup>S-labeled ECM or soluble ECM derived peak I proteoglycans. The incubation medium was centrifuged and the supernatant was analyzed by gel filtration on a Sepharose CL-6B column (0.9 × 30 cm) (refs. 33–37). Fractions (0.2 ml) were eluted with PBS and their radioactivity was measured<sup>7,10,33–37</sup>. Degradation fragments of HS side chains were eluted from Sepharose 6B at 0.5 < K<sub>av</sub> < 0.8 (peak II). A nearly intact HSPG was eluted next to just after the V<sub>0</sub> (K<sub>av</sub> < 0.2, peak I) (refs. 33–37). Each experiment was done at least three times and the variation of elution positions (K<sub>av</sub> values) did not exceed ±15%.

**Cloning of *hpa* cDNA.** The cDNA clones 257548 and 260138 were obtained from the I.M.A.G.E Consortium (Huntsville, Alabama). The cDNAs were originally cloned in *EcoRI* and *NotI* cloning sites in the plasmid vector pT3T7D-Pac. Marathon RACE (rapid amplification of cDNA ends) human placenta (polyA) cDNA composite was a gift from Y. Shiloh of Tel Aviv University. This composite is vector-free, as it includes reverse-transcribed cDNA fragments to which double, partially single-stranded adapters are attached on both sides<sup>50</sup>. Amplification of the 5' end of *hpa* cDNA PCR fragment was done according to the protocol provided by Clontech laboratories (Palo Alto, California). Gene-specific primers HPL229 and HPL171 were designed according to the sequence of the EST clones. They include nucleotides 933–956 and 876–897 of the heparanase cDNA sequence, respectively. The PCR program comprised 94 °C for 4 min, followed by 30 cycles of 94 °C for 40 s, 62 °C for 1 min, and 72 °C for 2.5 min. Amplification used Expand High Fidelity (Boehringer). The first amplification step used the AP1 primer and the gene-specific primer HPL229 (5'-GTAGTGATGCCATGTAAGTGAATC-3') and the second step used the nested 5' primer AP2 and a nested, gene-specific 3' primer (HPL171: 5'-GCATCTTAGCCGCTCTTCTTCG-3'). The resulting 900-bp PCR product was digested with *BfrI* and *PvuII*. The plasmid 257548 (*phpa1*) was digested with *EcoRI* followed by 'end-filling' and digestion with *BfrI*. The resulting fragment was ligated with PCR product that was digested with *BfrI*-*PvuII*. This resulted in pT3T7-Pac vector with the entire *hpa* cDNA (*phpa2*).

**DNA Sequencing.** Sequence determinations used vector-specific and gene-specific primers, with an automated DNA sequencer (model 373A; Applied Biosystems, Norwalk, Connecticut). Each nucleotide was read from at least two independent primers. Large-scale sequencing was done by Commonwealth Biotechnology, Richmond, Virginia.

**Expression of recombinant heparanase in insect cells.** High Five and Sf21 insect cell lines were maintained as monolayer cultures in SF900II-SFM medium (Life Technologies). Recombinant virus containing the *hpa* gene was constructed using the Bac to Bac system (Life Technologies). The transfer vector pFastBac was digested with *SaI* and *NotI* and ligated with a 1.7-kb fragment of *phpa2* digested with *XhoI* and *NotI*. The resulting plasmid was called pFast*hpa2*. Recombinant bacmid was generated according to the instructions of the manufacturer, with pFast*hpa2* and with pFastBac vector. The latter served as a negative control. Recombinant bacmid DNAs were transfected into Sf21 insect cells. Then, 5 d after transfection, recombinant viruses were collected and used to infect High Five insect cells (3 × 10<sup>6</sup> cells per T-25 flask). Cells were collected 2–3 days after infection, centrifuged and resuspended in a reaction buffer containing 20 mM phosphate citrate buffer, pH 6.2, and 50 mM NaCl. Cells were subjected to three cycles of freezing and thawing, and lysates were stored at –80 °C. Conditioned medium was stored at 4 °C.

**Screening of genomic libraries.** A human genomic library in Lambda phage EMBL3 SP6/T7 (Clontech) was screened. Plaques (5 × 10<sup>5</sup>) were plated at 5 × 10<sup>4</sup> plaque-forming units per plate on NZCYM agar/top agarose plates. Phages were absorbed on nylon membranes in duplicates (Qiagen). Hybridization was done at 65 °C in 5× SSC, 5× Denhart's, 10% dextran sulfate, 100 μg/ml salmon sperm and <sup>32</sup>P-labeled probe (10<sup>6</sup> cpm/μl). A 1.7-kb fragment, containing the entire *hpa* cDNA was labeled by random priming (Boehringer). After hybridization, membranes were washed once with 2× SSC, 0.1% SDS at 65 °C for 20 min, and twice with 0.2× SSC, 0.1% SDS at 65 °C for 15 min. Phage DNA was extracted using Lambda DNA extraction kit (Qiagen). The DNA fragment that fills the gap between the isolated lambda clones was cloned by PCR amplification from human genomic DNA using gene-specific primers derived from the terminal sequence of the lambda clones.

**Chromosomal localization.** Monochromosomal somatic cell hybrids were obtained from the HGMP Research Center (Hinxton, Cambridge, UK). Hybrid DNA (40 ng) was amplified with the gene-specific primers HPU 565 (5'-AGCTCTGTAGATGTGCTATACAC-3') and HPL 171 (see above).

**Computer analysis of sequences.** Homology searches used several computer servers and various databases. The Blast 2.0 service, at the NCBI server was used to screen the protein database swplus and DNA databases such as

GenBank, EMBL, and the EST databases. Sequence analysis and alignments were done using the DNA sequence analysis software package developed by the Genetic Computer Group (GCG) at the University of Wisconsin. The hydropathic profile was calculated by the Protein Hydrophilicity/Hydrophobicity Search and Comparison Server at the bioinformatics and biological computing unit at the Weizmann Institute of Science (Rehovot, Israel).

**Plasmids and transfection.** The heparanase cDNA was subcloned with the eukaryotic expression plasmid pcDNA3 (Invitrogen) at the *Hind*III and *Eco*R1 sites. Eb cells were grown in suspension ( $1 \times 10^6$  cells/ml) and a total of 5–20  $\mu$ g DNA and DOTAP transfection reagent (10  $\mu$ g DOTAP/ $\mu$ g DNA; 4.5-hour incubation; Boehringer) were used for transfection. Transfected cells were selected with 0.6 mg/ml G418 and stable populations of heparanase expressing cells were obtained by limiting dilution. Expression of heparanase was evaluated by RT-PCR and measurements of enzymatic activity. Pooled cell populations were inoculated subcutaneously into DBA/2 mice and survival rate and liver metastases were evaluated. The pcDNA3 heparanase plasmid was also used for transient transfection of low metastatic B16-F1 mouse melanoma cells. Transfected cells were intravenously inoculated into C57/BL mice and the number of lung metastases was determined 14 d afterwards<sup>10</sup>.

**RNA isolation and RT-PCR.** RNA was isolated with TRIzol (Life Technologies) according to the manufacturer's instructions and was quantitated by ultraviolet absorption. After reverse transcription of 500 ng total RNA by oligo(dT) priming, the resulting single stranded cDNA was amplified using TaqDNA polymerase and buffer (Promega). Oligonucleotide primers HPU-355 (5'-TTCGATCCCAAGAAGGAATCAAC-3') and HPL-229 (5'-GTAGTGATGCCATGTAACGAATC-3') were used. The PCR conditions were an initial denaturation of 4 min at 94 °C and subsequent denaturation for 45 s at 94 °C, annealing for 1 min at 60 °C and extension for 1 min at 72 °C (26 cycles). Aliquots of 10  $\mu$ l of the amplification products were separated by 1.5% agarose gel electrophoresis and visualized by ethidium bromide staining. Only RNA samples that gave completely negative results in PCR without reverse transcriptase were further analyzed.

**Expression pattern of the heparanase gene transcript (*in situ* hybridization).** RNA probes were transcribed and labeled by T7 RNA polymerase (for sense orientation) or T3 RNA polymerase (for antisense orientation) using DIG-UTP<sup>27</sup> labeling mixture (Boehringer). Probes were generated from T3T7-*Pac* plasmid containing 619-bp fragments of the human heparanase cDNA sequence inserted into the *Eco*R1-*Hind*III site. Final concentration for hybridization was 1  $\mu$ g/ml, according to the manufacturer's instructions for a non-radioactive *in situ* hybridization. Paraffin-embedded tissue sections were treated with 0.2 N HCl followed by proteinase K to expose the target RNA and with hybridization buffer to block nonspecific binding sites before the probe was added<sup>27</sup>. Hybridizations were incubated overnight at 45°. Slides were washed three times (1 h each) in 0.2 $\times$  SSPE at 50 °C, and were blocked by a blocking reagent (Boehringer). Detection was done by incubation overnight at room temperature with alkaline phosphatase-conjugated antibodies against DIG (Fab fragment, diluted 1:500; Boehringer). Alkaline phosphatase reaction was detected by NBT/BCIP reagents (Boehringer) according to the manufacturer's instructions.

**Antibodies against heparanase.** Monoclonal antibodies against heparanase were raised against a denatured fragment of heparanase expressed in *Escherichia coli*. A BamHI-*Kpn*I, 1.3-kb fragment encoding amino acids 130–543 was cloned into pRSET-C and overexpressed in *E. coli*. The fusion protein was purified by SDS-PAGE and injected into mice. Monoclonal antibodies were generated according to established protocols. Antibodies were screened for reactivity with recombinant heparanase produced in insect cells.

**Immunohistochemistry.** Fixed and paraffin-embedded tissue specimens were deparaffinized, rehydrated dematerialized for 3 min in a microwave oven and treated to block nonspecific staining. For this, sections were incubated for 30 min at 24 °C with 1% H<sub>2</sub>O<sub>2</sub> in methanol, followed by blocking for 30 min with 5% normal horse serum in PBS. Monoclonal antibodies against heparanase were added (1:50–1:200 dilution) for 16 h at 24 °C, followed

by incubation for 30 min at room temperature with biotinylated secondary horse-anti-mouse IgG antibodies and 30 min with avidin-biotin peroxidase conjugate (1:50 dilution) (Vectastain elite Universal kit: Vector Laboratories, Burlingame, California). Color was developed using Sigma Fast 3,3'-Diaminobenzidine tablet sets (Sigma) for 10 min followed by counterstain with Mayer's hematoxylin.

**Western blot analysis.** Cells were dissolved in lysis buffer containing 10 mM Tris-HCl, pH 7.4, 150 mM NaCl, 1 mM EDTA, 1% Triton-X100 and protease inhibitors (5  $\mu$ g/ml aprotinin, 1 mM phenylmethylsulfonyl fluoride, 10  $\mu$ g/ml leupeptin) for 30 min at 4 °C. After centrifugation (10,000g for 20 min at 4 °C), the protein content of the supernatants was measured. Lysates (50  $\mu$ g protein) were loaded and separated by 10% SDS-PAGE, and then transferred to Immobilon-P membrane (Millipore, Bedford, Massachusetts). Membranes were blocked and probed with monoclonal antibodies against heparanase in 1% BSA, 10 mM Tris-HCl, pH 7.5, 100 mM NaCl and 0.05% Tween-20. After being washed, blots were incubated with horseradish peroxidase-conjugated antibodies against mouse. Immunoreactive bands were detected by the enhanced chemiluminescence reagent using luminol and p-cumaric acid (Sigma). The light emitted by the chemical reaction was detected by exposure to Hyperfilm™ ECL (Amersham) for 30–60 s.

#### Acknowledgments

We thank D. Melamed, E. Feinstein, O. Yacoby-Zeevi, M. Ayal-Hershkovitz, E. Levi and Z. Rangini-Gueta for encouragement, discussions and assistance. This work was supported by grants from the Israel Science Foundation administered by the Israel Academy of Sciences and Humanities; The Israel Cancer Research Fund (ICRF), the GSF (German Forschungszentrum fur umwelt und gesundheit) (BMBF-MOS); and InSight.

RECEIVED 12 MARCH; ACCEPTED 20 APRIL 1999

- Kjellen, L. & Lindahl, U. Proteoglycans: structures and interactions. *Annu. Rev. Biochem.* **60**, 443–475 (1991).
- David, G. Integral membrane heparan sulfate proteoglycan. *FASEB J.* **7**, 1023–1030 (1993).
- Jackson, R.L., Busch, S.J. & Cardin, A.L. Glycosaminoglycans: Molecular properties, protein interactions and role in physiological processes. *Physiol. Rev.* **71**, 481–539 (1991).
- Wight, T.N., Kinsella, M.G. & Qwarnstrom, E.E. The role of proteoglycans in cell adhesion, migration and proliferation. *Curr. Opin. Cell Biol.* **4**, 793–801 (1992).
- Rapraeger, A.C. The coordinated regulation of heparan sulfate, syndecans and cell behavior. *Curr. Opin. Cell Biol.* **5**, 844–853 (1993).
- Wight, T.N. Cell biology of arterial proteoglycans. *Arteriosclerosis* **9**, 1–20 (1989).
- Vlodavsky, I., Fuks, Z., Bar-Ner, M., Ariav, Y. & Schirmacher, V. Lymphoma cell mediated degradation of sulfated proteoglycans in the subendothelial extracellular matrix: Relationship to tumor cell metastasis. *Cancer Res.* **43**, 2704–2711 (1983).
- Nakajima, M., Irimura, T., DiFerrante, D., DiFerrante, N. & Nicholson, G.L. Heparan sulfate degradation: relation to tumor invasion and metastatic properties of mouse B16 melanoma sublines. *Science* **220**, 611–613 (1983).
- Nakajima, M., Irimura, T. & Nicholson, G.L. Heparanase and tumor metastasis. *J. Cell. Biochem.* **36**, 157–167 (1988).
- Vlodavsky, I. *et al.* Inhibition of tumor metastasis by heparanase inhibiting species of heparin. *Invasion Metastasis* **14**, 290–302 (1995).
- Parish, C.R., Coombe, D.R., Jakobsen, K.B. & Underwood, P.A. Evidence that sulphated polysaccharides inhibit tumor metastasis by blocking tumor cell-derived heparanase. *Int. J. Cancer* **40**, 511–517 (1992).
- Lider, O. *et al.* Suppression of experimental autoimmune diseases and prolongation of allograft survival by treatment of animals with heparinoid inhibitors of T lymphocyte heparanase. *J. Clin. Invest.* **83**, 752–756 (1989).
- Willenborg, D. O. & Parish, C. R. Inhibition of allergic encephalomyelitis in rats by treatment with sulfated polysaccharides. *J. Immunol.* **140**, 3401–3405 (1988).
- Vlodavsky, I. *et al.* Expression of heparanase by platelets and circulating cells of the immune system: Possible involvement in diapedesis and extravasation. *Invasion Metastasis* **12**, 112–127 (1992).
- Graham, L.D. & Underwood, P.A. Comparison of the heparanase enzymes from mouse melanoma cells, mouse macrophages and human platelets. *Biochem. Mol. Biol.* **39**, 563–571 (1996).
- Ishai-Michaeli, R., Eldor, A. & Vlodavsky, I. Heparanase activity expressed by platelets, neutrophils and lymphoma cells releases active fibroblast growth factor from extracellular matrix. *Cell Reg.* **1**, 833–842 (1990).
- Vlodavsky, I., Bar-Shavit, R., Ishai-Michaeli, R., Bashkin, P. & Fuks, Z. Extracellular sequestration and release of fibroblast growth factor: a regulatory mechanism? *Trends Biochem. Sci.* **16**, 268–271 (1991).
- Eisenberg, S., Sehayek, E., Olivecrona, T. & Vlodavsky, I. Lipoprotein lipase enhances binding of lipoproteins to heparan sulfate on cell surfaces and extracellular matrix. *J. Clin. Invest.* **90**, 2013–2021 (1992).

19. Oosta, G.M., Favreau, L.V., Beeler, D.L. & Rosenberg, R.D. Purification and properties of human platelet heparitinase. *J. Biol. Chem.* **257**, 11249–11255 (1982).
20. Freeman, C. & Parish, C.R. Human platelet heparanase: Purification, characterization and catalytic activity. *Biochem. J.* **330**, 1341–1350 (1998).
21. Hoogewerf, A.J. *et al.* CXC chemokines connective tissue activating peptide-III and neutrophil activating peptide-2 are heparin/heparan sulfate-degrading enzymes. *J. Biol. Chem.* **270**, 3268–3277 (1995).
22. Gonzalo, V. *et al.* Partial sequence of human platelet heparitinase and evidence of its ability to polymerize. *Biochim. Biophys. Acta* **1429**, 431–438 (1999).
23. Jin, L., Nakajima, M. & Nicolson, G.L. Immunohistochemical localization of heparanase in mouse and human melanoma. *Int. J. Cancer* **45**, 1088–1095 (1990).
24. De Vouge, M.W. *et al.* Immunoselection of GRP94/Endoplasmic reticulum chaperone cell specific ggt11 library using antibodies directed against a putative heparanase amino-terminal peptide. *Int. J. Cancer* **56**, 286–294 (1994).
25. Goshen, R. *et al.* Purification and characterization of placental heparanase and its expression by cultured cytotrophoblasts. *Mol. Hum. Reprod.* **2**, 679–684 (1996).
26. Bar-Ner, M., Eldor, A., Wasserman, L., Matzner, Y. & Vlodavsky, I. Inhibition of heparanase mediated degradation of extracellular matrix heparan sulfate by modified and non-anticoagulant heparin species. *Blood* **70**, 551–557 (1987).
27. Even-Ram, S. *et al.* Thrombin receptor overexpression in malignant and physiological invasion processes. *Nature Med.* **8**, 909–914 (1998).
28. Larizza, L., Schirrmacher, V. & Pfluger, E. Acquisition of high metastatic capacity after *in vitro* fusion of a non-metastatic tumor line with a bone marrow derived macrophage. *J. Exp. Med.* **160**, 1579–1584 (1984).
29. Klein, U. & Figura, K.V. Substrate specificity of a heparan-sulfate degrading endoglucuronidase from human placenta. *Hoppe-Seyler's Z. Physiol. Chem.* **360**, 1465–1471 (1979).
30. Bame, K. J., & Robson K. Heparanases produce distinct populations of heparan sulfate glycosaminoglycans in Chinese hamster ovary cells. *J. Biol. Chem.* **272**, 2245–2251 (1997).
31. Sandback-Pikas, D., Li, J-P., Vlodavsky, I. & Lindahl, U. Substrate specificity of heparanases from human hepatoma and platelets. *J. Biol. Chem.* **273**, 18770–18777 (1998).
32. Pillarisetti, S. *et al.* Endothelial cell heparanase modulation of lipoprotein lipase activity. *J. Biol. Chem.* **272**, 15753–15759 (1997).
33. Yahalom, J., Eldor, A., Fuks, Z. & Vlodavsky, I. Degradation of sulfated proteoglycans in the subendothelial extracellular matrix by human platelet heparitinase. *J. Clin. Invest.* **74**, 1842–1849 (1984).
34. Bashkin, P., Razin, E., Eldor, A. & Vlodavsky, I. Degranulating mast cells secrete an endoglycosidase which degrades heparan sulfate in subendothelial extracellular matrix. *Blood* **75**, 2204–2212 (1990).
35. Matzner, Y. *et al.* Degradation of heparan sulfate in the subendothelial basement membrane by a readily released heparanase from human neutrophils. *J. Clin. Invest.* **76**, 1306–1313 (1985).
36. Naparstek, Y., Cohen, I.R., Fuks, Z. & Vlodavsky, I. Activated T lymphocytes produce a matrix-degrading heparan sulfate endoglycosidase. *Nature* **310**, 241–243 (1984).
37. Peretz, T. *et al.* Maintenance on extracellular matrix and expression of heparanase activity by human ovarian carcinoma cells from biopsy specimens. *Int. J. Cancer* **45**, 1054–1060 (1990).
38. Kleiner, D. E. & Stetler-Stevenson, W. G. Structural biochemistry and activation of matrix metalloproteinases. *Curr. Opin. Cell Biol.* **5**, 891–897 (1993).
39. Stetler-Stevenson, W. G. Type IV collagenases in tumor invasion and metastasis. *Cancer Metastasis Rev.* **9**, 289–303 (1990).
40. Mignatti, P. & Rifkin, D. B. Biology and biochemistry of proteinases in tumor invasion. *Physiol. Rev.* **73**, 161–195 (1993).
41. Bar-Ner, M. *et al.* Sequential degradation of heparan sulfate in the subendothelial extracellular matrix by highly metastatic lymphoma cells. *Int. J. Cancer* **35**, 483–491 (1985).
42. Vlodavsky, I. *et al.* in *Tumor Angiogenesis* (eds. Lewis, C.E., Bicknell, R & Ferrara, N.) 125–140 (Oxford University Press, Oxford, UK, 1997).
43. Vlodavsky, I., Bar-Shavit, R., Korner, G. & Fuks, Z. in *Basement Membranes: Cellular and Molecular Aspects* (eds. Rohrbach, D.H. & Timpl, R.) 327–343 (Academic, Orlando, Florida, 1993).
44. Yayon, A., Klagsbrun, M., Esko, J.D., Leder, P. & Ornitz, D.M. Cell surface, heparin-like molecules are required for binding of basic fibroblast growth factor to its high affinity receptor. *Cell* **64**, 841–848 (1991).
45. Miao, H-Q., Ornitz, D. M., Ingorn, E., Ben-Sasson, S. A. & Vlodavsky I. Modulation of fibroblast growth factor-2 receptor binding, dimerization, signaling, and angiogenic activity by a synthetic heparin-mimicking polyanionic compound. *J. Clin. Invest.* **99**, 1565–1575 (1997).
46. Vlodavsky, I. *et al.* Endothelial cell-derived basic fibroblast growth factor: Synthesis and deposition into subendothelial extracellular matrix. *Proc. Natl. Acad. Sci. USA* **84**, 2292–2296 (1987).
47. Vlodavsky, I. & Christofori, G. in *Antiangiogenic Agents in Cancer Therapy* (ed. Teicher, B.A.) 93–118 (Humana, Totowa, New Jersey, 1998).
48. Soule, H.D. *et al.* Isolation and characterization of a spontaneously immortalized human breast epithelial cell line, MCF-10. *Cancer Res.* **50**, 6075–6086 (1990).
49. Vlodavsky, I. in *Current protocols in Cell Biology*, Vol. 1, Suppl. 1 (eds. Bonifacino, J.S., Dasso, M, Harford, J.B, Lippincott-Schwartz, J & Yamada, K.M.) 10.4.1–10.4.14 (John Wiley & Sons, New York, New York, 1999).
50. Savitsky, K. *et al.* Ataxia-telangiectasia: structural diversity of untranslated sequences suggests complex post-translational regulation of ATM gene expression. *Nucleic Acids Res.* **25**, 1678–1684 (1997).